

# Structural, elastic, optoelectronic and optical properties of CuX (X= F, Cl, Br, I): A DFT study

HAMID ULLAH<sup>\*,a</sup>, A. H. RESHAK<sup>b,c</sup>, KALSOOM INAYAT<sup>a</sup>, R. ALI<sup>a</sup>, G. MURTAZA<sup>d</sup>, SHERAZ<sup>e</sup>, S. A. KHAN<sup>f</sup>, H. U. DIN<sup>f</sup>, Z. A. ALAHMED<sup>g</sup>

<sup>a</sup>Department of Physics, Government Post Graduate Jahanzeb College, Saidu Sharif Swat, Pakistan

<sup>b</sup>New Technologies - Research Center, University of West Bohemia, Univerzitni 8, 306 14 Pilsen, Czech Republic

<sup>c</sup>Center of Excellence Geopolymer and Green Technology, School of Material Engineering, University Malaysia Perlis, 01007 Kangar, Perlis, Malaysia

<sup>d</sup>Department of Physics, Material Modeling Lab, Isalmia College University Peshawar, Pakistan

<sup>e</sup>Department of Physics, Balochistan University of information technology, engineering and management sciences, Pakistan

<sup>f</sup>Department of Physics, Hazara University Mansehra, Pakistan

<sup>g</sup>Department of Physics and Astronomy, King Saud University, Riyadh 11451, Saudi Arabia

The structural, elastic, electronic and optical properties of copper halides **CuX (X= F, Cl, Br, I)** are performed by using the full-potential linearized augmented plane wave (FP-LAPW) method within density functional theory (DFT). The exchange correlation potential was described by generalized gradient approximation (GGA) and Engel-Vosko generalized gradient approximation (EV-GGA). For better electronic properties we have used the modified Becke–Johnson (mBJ) potential. Copper Halides, **CuX (X= F, Cl, Br, I)** have zinc-blend structure (B3) and shows direct band gap. The results obtained for band structure using mBJ potential shows a significant improvement over previous theoretical work and gives closer values to the experimental available data. The elastic constants values have also been analyzed for these materials. In the elastic constants it has been found that CuF and CuBr show brittle nature while CuCl and CuI show ductile behaviour. Optical parameters, like the dielectric constant, refractive indices, reflectivity, optical conductivity and absorption coefficient has also been calculated and presented.

(Received December 26, 2013; accepted November 13, 2014)

**Keywords:** DFT, mBJ potential, Elastic, optoelectronic, Optical properties

## 1. Introduction

Copper halides have been studied for several decades [1-3] but the importance of IB-VIIA semiconductors are still growing because of the potential applications occurring from the restricted excitons in micro-crystals made of these materials [4]. The copper halides crystallize in the zinc blend lattice (space group F-43m) and are tetrahedral coordinated semiconductors. Cu atom is located at position (0, 0, 0), while X (F, Cl, Br, I) atoms are located at (1/4, 1/4, 1/4) positions. The electronic configuration of zinc blend structure is derived from  $sp^3$ - $sp^3$  configuration while the valence bands of copper halides are due to  $sp^3$ - $sd^3$ . As a result of the  $p$ - $d$  hybridization considerably changes physical properties of copper halides are considerably different compared with other members of  $A^N B^{8-N}$  series. B. Amrani *et al* [5] performed under pressure calculations on these materials and found that they transform from the zinc-blend (B3) to the rocksalt (B1) structure. Experimental studies [6-8] have revealed that CuCl, CuBr and CuI adopt the rocksalt structure at a pressure around in the region of 10 GPa, though the zinc blende-rocksalt transition occurs via several intermediate structures of lower symmetry. According to Amrani *et al*, the most interesting feature of the copper halides is the occurrence of a filled  $d^{10}$ -shell.

The  $d$ -electrons in the copper and silver halides are part of the uppermost valence bands and, therefore, influence the electronic properties of these compounds. The I–VII semiconductors exhibit nonlinear optical properties. These materials are promising candidates for photosensitive and semiconducting materials, hence attract much attention.

A wide range of theoretical studies have been executed on copper halides. The commonly used pseudo-potential method made less useful for the calculation of the energy bands of normal zinc blend semiconductors by the presence of  $d$  levels. The tight binding method was used to perform the calculation of IB-VIIA compounds by Song [9] and Khan [10]. The mixed tight binding plane wave (MTB-PW) calculation were made by Calabrese and Fowler [11] which have been critically reviewed by Goldman [12], Zunger and Cohen [13], Kleinman and Medinck [14] and Kunz and Weidman [15]. Furthermore calculation had been done by the linear muffin-tin orbital (LMTO) method [16,17]. The calculations for IB-VIIA compounds among available pseudo-potential by Wang *et al*. [18], Smith [19] and Hsueh *et al*. [20]. Despite from numerous theoretical work, the detail are still incomplete because the predicted band gaps are still much lower than the experimental measurements. Therefore, it is necessary to investigate the physical properties of copper halides in detail.

To calculate the band structure of comparatively localized  $d$  valence electron, it is most suitable to use method which stresses the atomic nature of the wave function. The objective of this paper is to apply the full-potential linearized augmented plane wave (FP-LAPW) method [21] for calculating the structural, elastic, electronic and optical properties of CuX (X= F, Cl, Br, I).

We have presented here the structural, elastic, electronic and optical properties for CuX (X= F, Cl, Br, I). Our calculated values for the structural and electronic properties for these materials are much better than the previous work and are very closer to the experimental results. Here in this work we have included Copper fluoride (CuF) and to the best of our knowledge there is no previous work has been done upon it, which can be use as a reference for future investigations. We have also calculated the elastic constants values along with Young's modulus  $E$  (in GPa), shear modulus  $G$  (in GPa), Poisson's ratio  $\nu$ , anisotropy factor  $A$  and  $B/G$  ratio which has not been done may not be done before this. We have also calculated the electron density, which is an important bonding property for a material.

## 2. Computational details

The calculations are carried out by using the FP-LAPW [21] method as implemented in Wien2k package [22]. The exchange correlation potential was described by generalized gradient approximation of Wu and Cohen (WC-GGA) [23], Engel and Vosko (EV-GGA) [24-44], and modified Becke-Johnson potential (mBJ) [17]

potential for the better electronic properties. The last two approximations are used to overcome the well-known GGA underestimation of the energy band gap. The spherical harmonics inside non-overlapping muffin-tin (MT) spheres surroundings the atomic spheres are expanded up to  $l_{\max} = 9$ . The plane wave cut-off of  $R_{\text{MT}}K_{\max} = 8.5$ , was chosen for the expansion of wave functions in the interstitial region. Meshes of 1000  $\mathbf{k}$ -points are used for the irreducible wedge of Brillouin zone (BZ). The self-consistent calculations are converged since the total energy of the system is stable within  $10^{-3}$ Ry.

## 3. Results and discussions

### 3.1. Ground state properties

The calculated total energy of CuX (X=F,Cl, Br, I) unit cell is a function of volume in zinc blend phase. To calculate the ground state properties of CuX (X= F, Cl, Br, I), the volume was optimized by the Murnaghan equation of states [25]. The equilibrium volume, bulk modulus, derivative of the bulk modulus with some theoretical and experimental results is given in Table 1. It is clear from the previous work that both of the local density approximation (LDA) and GGA underestimate the lattice parameters while our calculated results using EV-GGA and mBJ are in good agreement with the experimental data and other calculated results. From lower to higher atomic number the bulk modulus and energy decreases, while the lattice constants increases as we move from CuF to CuI for zinc blend phase.

Table 1. Calculated ground state properties of CuX (X= F, Cl, Br, I) using mBJ along with experimental and other theoretical work.

Compounds	Properties	Present Calculation		Experimental	Other Work	
		EV-GGA	mBJ		LDA/GGA	
CuF	$a_0$	4.87	4.77	-	-	-
	$E_0$	-3510.71	-3506.5191	-	-	-
	B	77.75	78.56	-	-	-
	$B'$	7.070	5.11	-	-	-
CuCl	$a_0$	5.45	5.324	5.424 <sup>b</sup>	5.246 <sup>a</sup> , 5.273 <sup>b</sup>	
	$E_0$	-4234.25	-4229.1			
	B	49.5727	63.2804	38.1 <sup>b</sup> , 39.8 <sup>c</sup> 54.5 <sup>d</sup>	48.38 <sup>a</sup>	
	$B'$	5.00	5.00	4 <sup>b</sup>	5.196 <sup>a</sup>	
CuBr	$a_0$	5.76	5.6215	5.695 <sup>b</sup>	5.744 <sup>a</sup> , 5.689 <sup>i</sup>	
	$E_0$	-8525.25	-8517.2			
	B	42.6095	54.8466	36.6 <sup>b</sup>	43.528 <sup>a</sup>	
	$B'$	5.00	5.00	4 <sup>b</sup>	5.1 <sup>a</sup>	
CuI	$a_0$	6.11	5.965	6.054 <sup>b</sup>	5.885 <sup>a</sup> , 6.082 <sup>j</sup>	
	$E_0$	-7550.95	-17540			
	B	44.6988	40.1147	36.6 <sup>b</sup> , 31 <sup>e</sup>	39.447 <sup>a</sup>	
	$B'$	5.00	5.00	4 <sup>b</sup>	4.704 <sup>a</sup>	

a[5], b[26], c[27], d[28], e[29], h[20], i[30], j[1]

#### 3.1.1 Elastic properties

The crystal properties like dynamical and mechanical properties are explained easily by elastic constants; it

explicitates material properties under stress i.e when deformation is produced in its shape and then regains its original shape after releasing stress [31]. Some valuable information like stability and stiffness of a material are

easily explained through this phenomenon. We have used *ab-initio* method for the calculation of the elastic moduli ( $C_{ij}$ ) by calculating stress tensor components for small strains, using Charpin's method implemented in the WIEN2K simulation package. We have calculated independent elastic parameters,  $C_{11}$ ,  $C_{12}$  and  $C_{44}$  for the complete explanation of mechanical properties of CuX (X= F, Cl, Br, I) in the zinc blend (B3) phase.

Table 2 clarifies that the unidirectional elastic constant  $C_{11}$  are higher than that of  $C_{44}$  in zinc blend phase performed with WC-GGA potential. This shows that material having larger difference  $C_{11}-C_{44}$  presents a weaker resistance to the pure shear deformation. In a cubic structures the condition for mechanical stability leads to the following reaction on elastic constants [31]:

$$(1/3)(C_{11}+2C_{12}>0; C_{44}>0; (C_{11}-C_{12})>0 \quad (1)$$

Hence the mechanical condition for these materials are fulfilled and presenting the elastic stability of these compounds.

In engineering sciences, elastic anisotropy of a material play a vital role, it has the possibility to detect micro-cracks in a material [32] due to high correlativity. The anisotropy factor  $A$  is calculated from the elastic constant of these compounds, which can be calculated from the equation given below;

$$A= 2C_{44}/ (C_{11} - C_{12}) \quad (2)$$

Material having anisotropy factor  $A$  smaller or greater than 1, indicates anisotropy behavior, while show isotropic behavior if the value of  $A$  is equal to 1 [31]. It is clear from Table 2, that all the listed compounds show anisotropic behaviour in the zinc blend (B3) phase.

From the elastic constants  $C_{ij}$  we can also calculate shear modulus ( $G$ ), Young's modulus ( $E$ ), Pugh's index of

ductility ( $B/G$ ) and Poisson's ratio  $\nu$ , using Voigt–Reus–Hill approximations and the following expressions [33–36]:

$$E = \frac{9BG}{3B + G} \quad (3)$$

$$G_R = \frac{5C_{44}(C_{11}-C_{12})}{4C_{44}+3C_{11}-C_{12}} \quad (4)$$

$$G_V = \frac{1}{5}(C_{11}-C_{12}+3C_{44}) \quad (5)$$

The shear modulus  $G$  is given by:

$$G = G_V - G_R \quad (6)$$

The stiffness of materials depends upon the Young's modulus ( $E$ ) of the material, higher the Young's modulus ( $E$ ) stiffer will be the materials. It is clear from Table 2 that CuF with  $E= 77.30$ , is much stiffer than the remaining listed compounds in this table. Important property of the elastic constant parameters is to calculate the ductility and brittleness of a material. Different parameters (Cauchy pressure, Pugh's index, Poisson's ratio) are used for calculating the brittleness and ductility of material. We are using here the Pugh's index of ductility for the compounds CuX (X= F, Cl, Br, I).

The ductility index is calculated by the pugh's ( $B/G$ ) [37] ratio. The critical number of  $B/G$  ratio is 1.75 which separates ductile from the brittle material. Greater the  $B/G$  ratio, high will be the ductility and smaller the  $B/G$  ratio, brittle will be the material [31]. It's clear from the  $B/G$  ratio in Table 2 that, CuF and CuBr show brittle nature while CuCl and CuI show ductile behaviour.

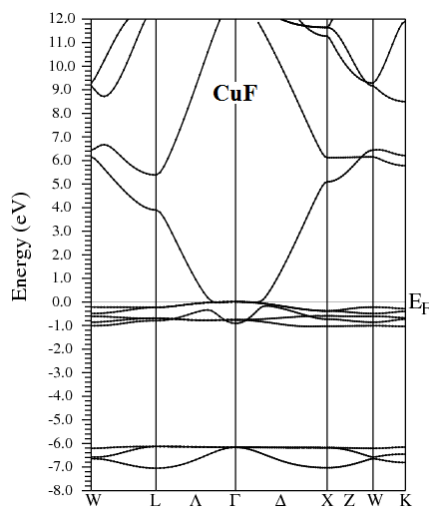
Table 2. Calculated elastic constants  $C_{ij}$  (in GPa), Young's modulus  $E$  (in GPa), shear modulus  $G$  (in GPa), Poisson's ratio  $\nu$ , anisotropy factor  $A$  and  $B/G$  ratio for CuX (X= F, Cl, Br, I), has been presented along with other theoretical and experimental results.

		$C_{11}$	$C_{12}$	$C_{44}$	$E$	$G$	$\nu$	$A$	$B/G$
CuF	This work	91.09	8.24	26.09	77.30	31.42	0.23	0.63	1.51
	Theory	-	-	-	-	-	-	-	-
	Experimental	-	-	-	-	-	-	-	-
CuCl	This work	58.34	73.15	55.42	10.45	3.56	0.46	-7.48	15.8
	Theory	46.47 <sup>k</sup> , 48.57 <sup>k</sup> ,48.6 <sup>l</sup> , 45.28 <sup>m</sup> , 47 <sup>n</sup> , 14.9 <sup>o</sup> 45.4 <sup>p</sup>	34.82 <sup>k</sup> , 35.87 <sup>k</sup> , 34.8 <sup>l</sup> , 30.91 <sup>m</sup> , 36.2 <sup>n</sup> , 74.1 <sup>o</sup> 36.9 <sup>p</sup>	13.79 <sup>k</sup> ,13.21 <sup>k</sup> ,15.3 <sup>l</sup> , 12.19 <sup>m</sup> , 55.3 <sup>o</sup> 14.9 <sup>p</sup>	-	-	-	-	-
	Experimental	-	-	-	-	-	-	-	-
CuBr	This work	70.44	35.03	40.16	72.79	28.92	0.25	2.26	1.73
	Theory	64.42 <sup>k</sup> , 53.99 <sup>k</sup> , 44 <sup>l</sup> , 43.5 <sup>n</sup>	50.39 <sup>k</sup> , 40.67 <sup>k</sup> , 32.6 <sup>l</sup> , 34.9 <sup>n</sup>	7.53 <sup>k</sup> , 6.85 <sup>k</sup> , 12.3 <sup>l</sup>	-	-	-	-	-
	Experimental	-	-	-	-	-	-	-	-
CuI	This work	39.91	43.09	45.09	30.70	11.11	0.38	-28.4	3.90
	Theory	72.39 <sup>k</sup> ,50.7 <sup>l</sup> , 5 <sup>k</sup> , 45.2 <sup>l</sup> , 41.3 <sup>q</sup> , 45.1 <sup>n</sup> , 52.8 <sup>l</sup> , 45.1 <sup>p</sup>	51.68 <sup>k</sup> ,33.80 <sup>k</sup> , 32.2 <sup>l</sup> , 32.1 <sup>q</sup> , 30.7 <sup>n</sup> , 34.4 <sup>l</sup> , 30.7 <sup>p</sup>	22.72 <sup>k</sup> , 9.50 <sup>k</sup> , 10.4 <sup>l</sup>	-	-	-	-	-
	Experimental	-	-	-	-	-	-	-	-

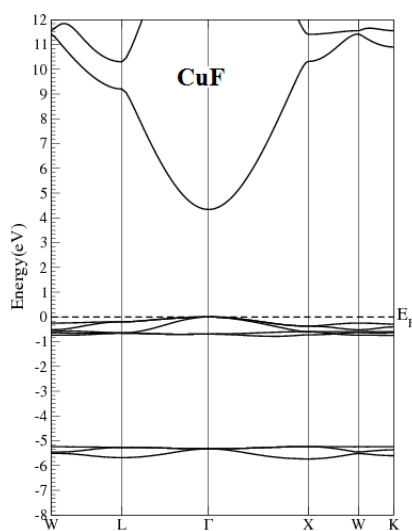
k[5],l[1],m[38],n[39],o[40],p[41],q[42]

### 3.2 Electronic properties

We have calculated the band structure of the CuX (X= F, Cl, Br, I) by using EV-GGA and mBJ potentials. It is clear from Fig. 1 (a), by using EV-GGA potential that the valence and conduction bands for CuF overlapped with each other at Fermi level ( $E_F$ ), indicating the metallic nature of CuF. However when we applied the mBJ potential, the valence and conduction bands are shifted away from each other, leading to open a direct energy gap at  $\Gamma$ - $\Gamma$  symmetry point. This improvement in the energy band gap value is attributed to the better predicting ability of  $d$  states of elements by mBJ. The calculated band gap value of CuF is presented in Table 3. To the best of our knowledge there is no experimental and theoretical data available to compare our results for CuF. Thus we have expected that this work can be used as a reference for further investigation of physical properties of CuF.



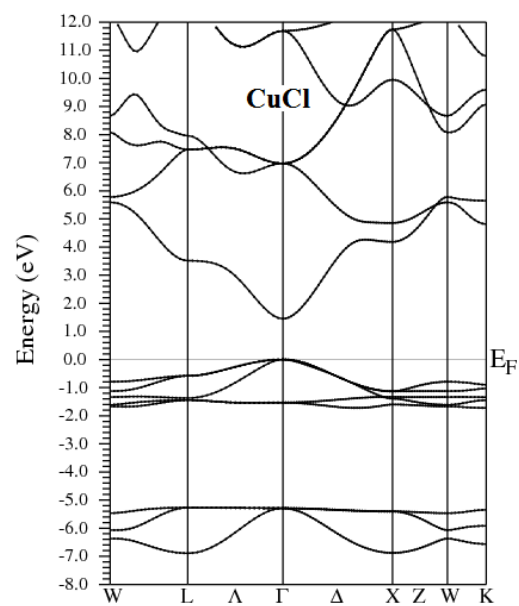
(a)



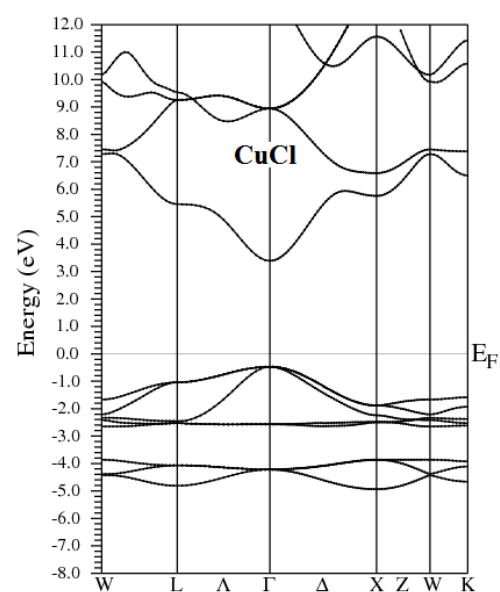
(b)

Fig. 1(a). Calculated band structure of CuF;  
(a) EV-GGA, (b) mBJ.

The calculated electronic band structure of CuCl, CuBr and CuI using EV-GGA and mBJ potential are shown in Fig.(2, 3 and 4). These figures clearly show that the top of the valence band and bottom of the conduction band are located at  $\Gamma$ - $\Gamma$  symmetry point, hence CuCl, CuBr and CuI have direct band gap nature. Hence these materials are useful for optoelectronic devices applications. The theoretical results and the experimental data of the energy band gap of CuCl, CuBr and CuI are presented in Table 3. This clearly shows that our calculated values are very close to the experimental data and much better than the previous theoretical work.



(a)



(b)

Fig. 2. Calculated band structure of CuCl;  
(a) EV-GGA, (b) mBJ.

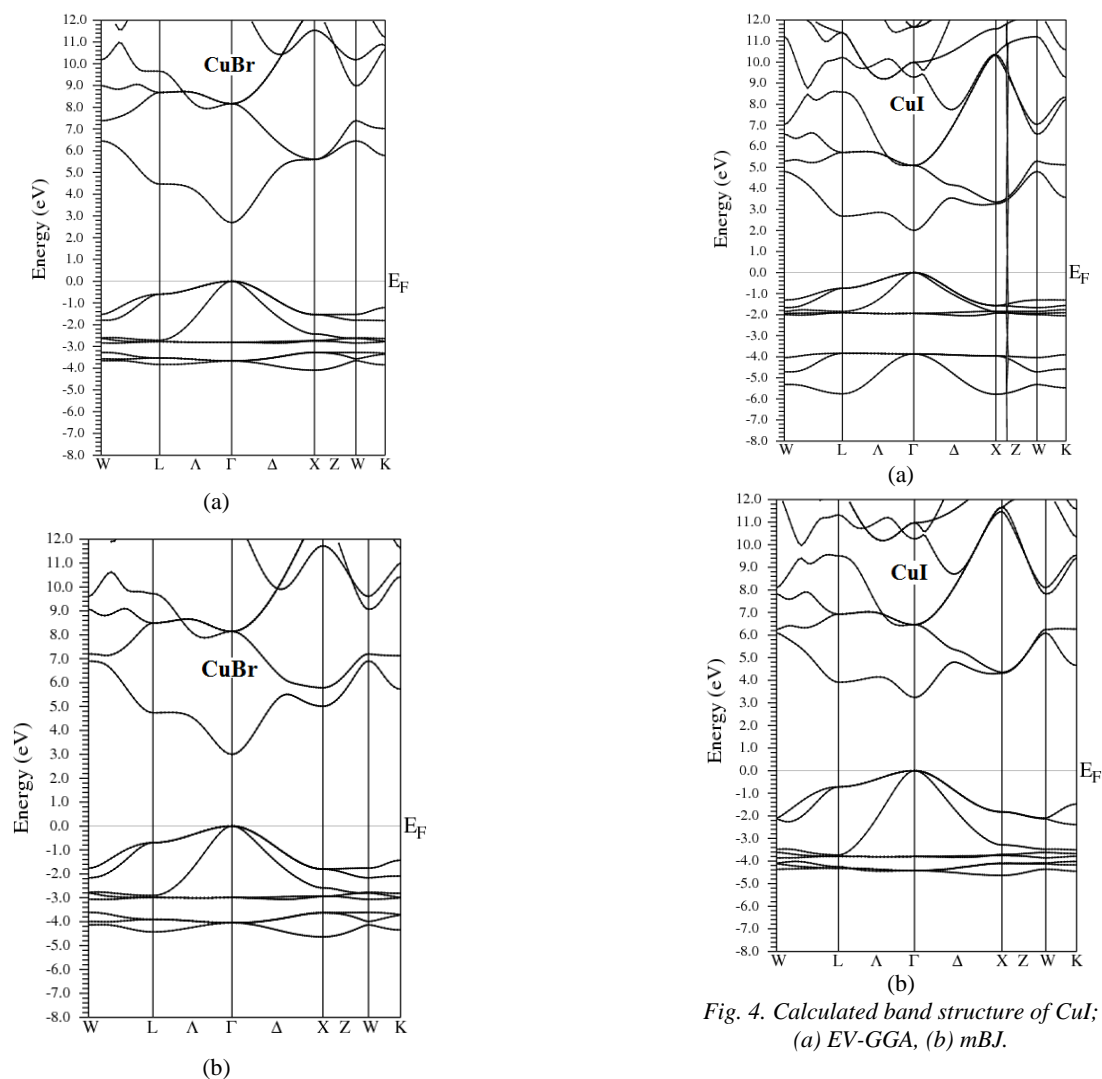


Fig. 3. Calculated band structure of CuBr ;  
(a) EV-GGA, (b) mBJ.

Fig. 4. Calculated band structure of CuI;  
(a) EV-GGA, (b) mBJ.

In the light of these results it is obvious that our calculated energy band structures using EV-GGA and mBJ are improved than the previously calculated energy band gaps by LDA and GGA and very close to the experimental results. That is attributed to the fact that both of EV-GGA and mBJ potential are more effective and producing better band splitting than LDA and GGA [43,44] and hence they bring the energy band gap closer to the experimental one.

Table 3. Calculated energy band gap values for CuX (X= F, Cl, Br, I) in ZB structure in comparison to the other theoretical works and available experimental data.

Compounds	Energy band structures (eV)			
	Present Work		Experimental	Other Calculations
	EV-GGA	mBJ		LDA/ GGA
CuF	Metallic	4.4	-	-
CuCl	1.22	3.40	3.40 <sup>a</sup>	0.538 <sup>f</sup> , 0.509 <sup>g</sup>
CuBr	2.7	3.00	3.05 <sup>b</sup> , 3.09 <sup>c</sup>	0.445 <sup>f</sup> , 0.418 <sup>g</sup>
CuI	2.00	3.10	3.115 <sup>d,e</sup>	1.118 <sup>f</sup> , 1.077 <sup>g</sup>

a[3], b[2], c[17], d[45], e[12], f[4], g[5]

### 3.2.1 Density of states (DOS)

Band structure can be further explored by the density of states (DOS). We have calculated the total and partial densities of states for CuX (X= F ,Cl, Br, I) compounds in the zinc blende (B3) phase using mBJ potential as shown in Fig. 5(a,b,c), 6(a,b,c), 7(a,b,c), 8(a,b,c). It is clear from the plots that the valence band (VB) shifts towards Fermi level with the change of anion from F to I in CuX. This band is mainly composed of Cu-d and X-p states near the Fermi level. Above the Fermi level is composed of mixture of *s,p,d* states. From Fig. 5(a,b,c), 6(a,b,c), 7(a,b,c), 8(a,b,c), it is seen that Cu-d and X-p states mainly contribute in the first band, while in the second band (CB) the *s,d* states of CuX are rarely involved.

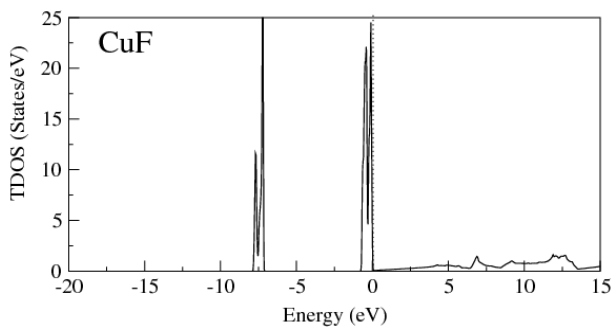


Fig. 5(a). Calculated total densities of states of CuF.

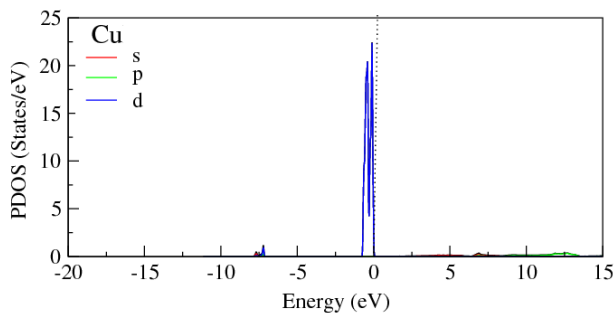


Fig. 5 (b). Calculated partial densities of states of Cu.

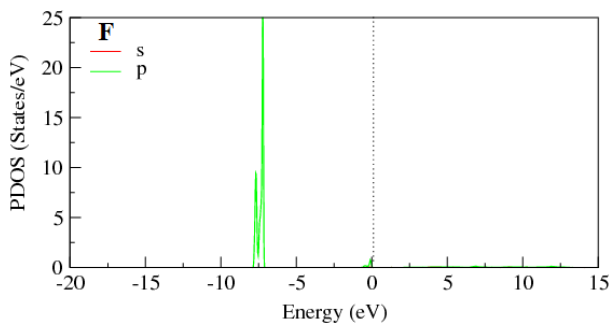


Fig. 5(c). Calculated partial densities of states of F.

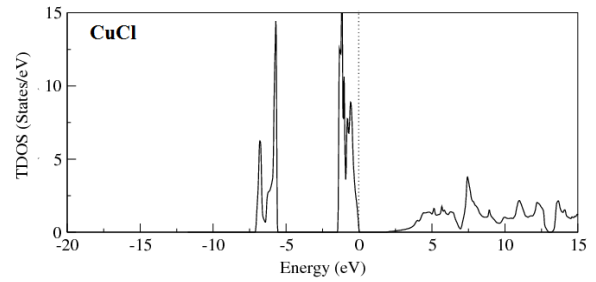


Fig. 6 (a). Calculated total densities of states of CuCl.

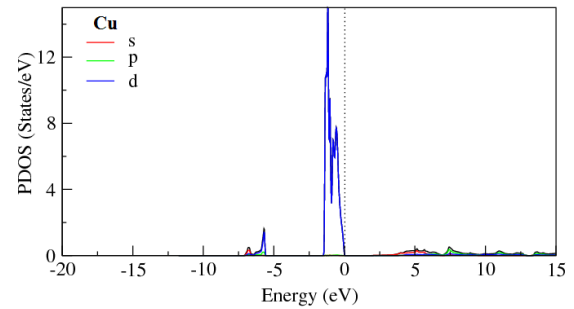


Fig. 6 (b). Calculated partial densities of states of Cu.

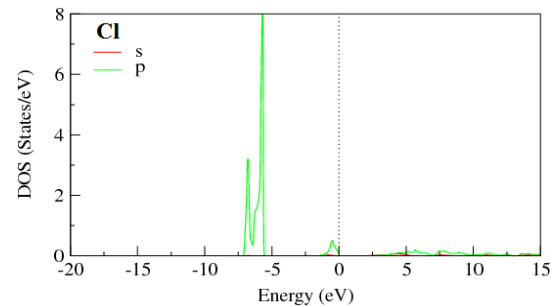


Fig. 6 (c). Calculated partial densities of states of Cl.

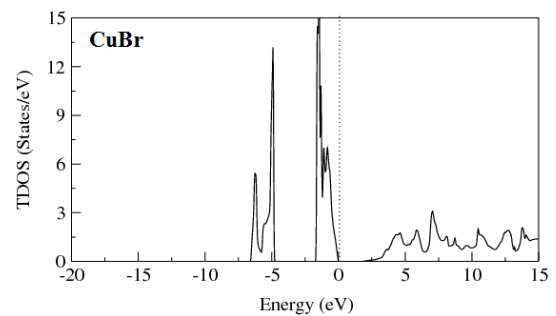


Fig. 7 (a). Calculated total densities of states of CuBr.

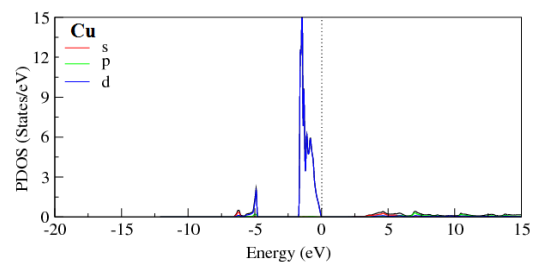


Fig. 7 (b). Calculated partial densities of states of Cu.

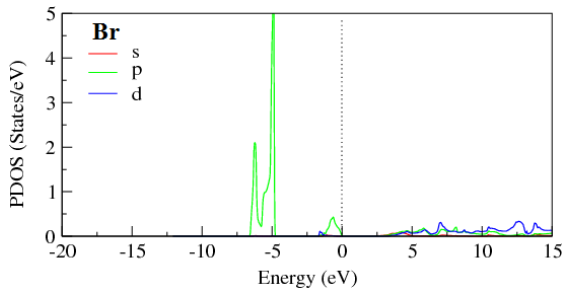


Fig. 7 (c). Calculated partial densities of states of Br.

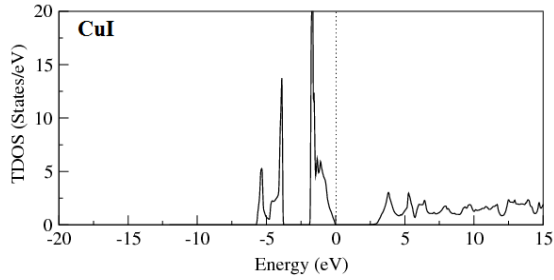


Fig. 8 (a). Calculated total densities of states of CuI.

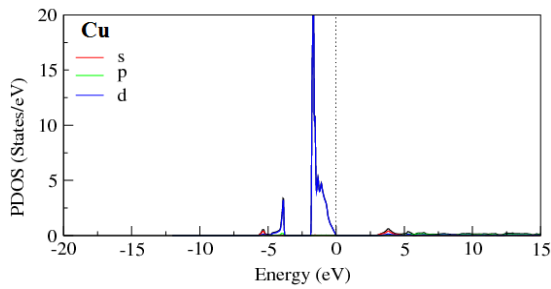


Fig. 8 (b). Calculated partial densities of states of Cu.

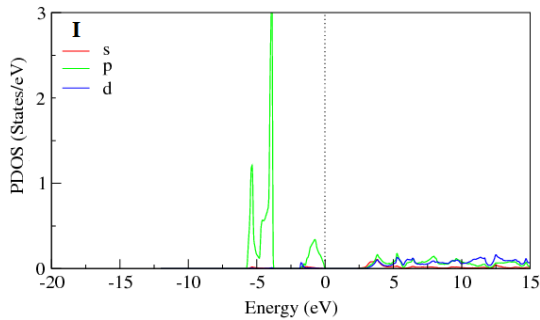
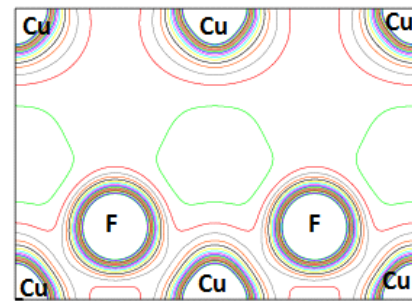


Fig. 8 (c). Calculated partial densities of states of I.

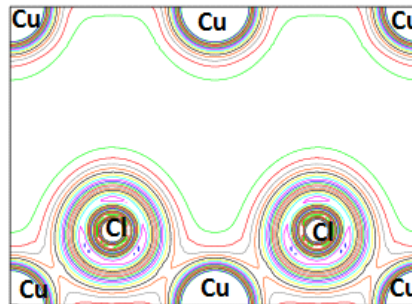
### 3.2.2 Electron charge density

The charge density distribution among the atom explains the bonding nature of material. The sharing of charges between cation and anion shows covalent bonding nature, while the transfer of charge among them shows ionic bonding nature. The charge density plots of CuX (X= F, Cl, Br, I) compounds in (1 1 0) plane are given in Fig. 9a-d. It is clear that F shows covalent nature with Cu. The remaining compounds CuCl, CuBr and CuI shows covalent nature among anion-anion and anion-cation atoms.

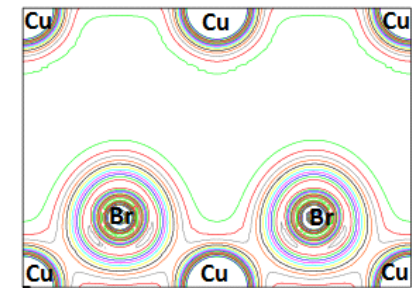
It is cleared from the figure that the charge is uniformly shared among cation Cu anion F. Hence the bonding in copper halides is more covalent. the Fig. shows that the Cu and F atom do not share the charges, due to the greater distance they only disturb the charge density contour round each other. When we replace F by Cl and Br then it makes strong covalent bonding with Cu atom. If we replace F by I atom, a weak covalent bond is making as compared to Cu-Cl and Cu-Br. However, the charge sharing among the copper cation is not seen in CuF, while it is seen in the other three compounds. Which shows the ionic bonding in CuF while covalent bonding in the other compounds.



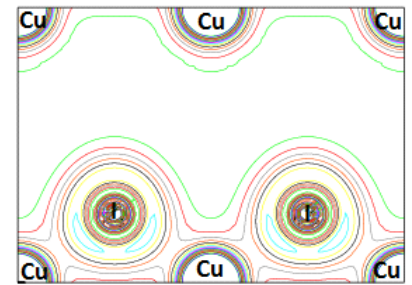
(a) Electron density plot of CuF



(b) Electron density plot of CuCl



(c) Electron density plot of CuBr



(d) Electron density plot of CuI

Fig. 9. Calculated charge density plots of CuX (X= F, Cl, Br, I) compounds in (1 1 0) plane.

### 3.2.3. Optical properties

The dielectric function of the electron gas which is strongly depends upon the frequency has an important effect on the physical properties of solids. It explains the combined excitations of the Fermi sea; for example the volume and surface plasmons. The dielectric function of a crystal depends on the electronic band structure, and it is investigated by optical spectroscopy which is a powerful tool to determine the band behaviour of solids. It consists of two parts i.e. real part and imaginary part [46]

$$\varepsilon(\omega) = \varepsilon_1(\omega) + i\varepsilon_2(\omega) \quad (7)$$

In momentum representation the dielectric function was calculated, which requires matrix elements of momentum  $p$  in occupied and unoccupied eigenstates. The imaginary part of the dielectric function  $\varepsilon_2(\omega)$  may be calculated by using relation [46].

$$\varepsilon_2(\omega) = \frac{8}{2\pi\omega^2} \sum_{m'} \int_{BZ} |P_{m'}(k)|^2 \frac{dS_k}{\nabla\omega_{m'}(k)} \quad (8)$$

$\varepsilon_2(\omega)$  depends on the joint density of states ( $\omega_{m'}$ ), and  $P_{m'}$  be the momentum matrix element. The real part  $\varepsilon_1(\omega)$  can be obtained from the imaginary part  $\varepsilon_2(\omega)$  by Kramers-Kronig equation [46]

$$\varepsilon_1(\omega) = 1 + \frac{2}{\pi} P \int_0^{\infty} \frac{\omega' \varepsilon_2(\omega')}{\omega'^2 - \omega^2} d\omega' \quad (9)$$

The refractive index  $n(\omega)$  can be directly calculated by the relation:

$$n(\omega) = \frac{1}{\sqrt{2}} \left[ \left\{ \varepsilon_1(\omega)^2 + \varepsilon_2(\omega)^2 \right\}^{1/2} + \varepsilon_1(\omega) \right]^{1/2} \quad (10)$$

$$k(\omega) = \frac{1}{\sqrt{2}} \left[ \left\{ \varepsilon_1(\omega)^2 + \varepsilon_2(\omega)^2 \right\}^{1/2} - \varepsilon_1(\omega) \right]^{1/2} \quad (11)$$

We may presume that  $k(\omega)$  is very small, when the medium is a weak absorber, so that

$$n = \sqrt{\varepsilon_1} \quad (12)$$

and 
$$k = \frac{\varepsilon_2}{2n} \quad (13)$$

From the above equation it is clear that the refractive index is determined by the real part of the dielectric function, while absorption coefficient by imaginary part of the dielectric functions.

The frequency dependent reflectivity can be calculated by using the above optical parameters  $n(\omega)$  and  $k(\omega)$  by using the following equation:

$$R(\omega) = \frac{|\tilde{n} - 1|}{|\tilde{n} + 1|} = \frac{(n-1)^2 + k^2}{(n+1)^2 + k^2} \quad (14)$$

Also the absorption coefficient can be determined from the dielectric function [47]:

$$\alpha(\omega) = 2\omega k(\omega) = \sqrt{2}\omega \left[ \left\{ \varepsilon_1(\omega)^2 + \varepsilon_2(\omega)^2 \right\}^{1/2} - \varepsilon_1(\omega) \right]^{1/2} \quad (15)$$

The absorption coefficient from Beer's law [35]:

$$\alpha = \frac{2k\omega}{c} = \frac{4\pi k}{c} \quad (16)$$

Fig. 10a-d, is the imaginary part of the dielectric function of CuX (X= F, Cl, Br, I) for the given energy ranges. The edge of the optical absorption in CuX (X= F, Cl, Br, I) take place at around 3.8 eV, 3.3 eV, 1.8 eV and 2.4 eV, respectively. The edge of the optical absorption occurs at  $\Gamma$  point of the BZ between the valence and conduction band, these are the threshold for the direct optical transition. This point is known as the fundamental absorption edge. Fig. 10a-d, also shows that CuX (X= F, Cl, Br, I) have a strong absorption between 3.5 eV to 18 eV and 13 eV for CuF and CuCl, while from 3.0 eV to 11 eV for CuBr and CuI respectively.

Fig. 10a-d, illustrated the real parts of the dielectric function  $\varepsilon_1(\omega)$  for CuX (X= F, Cl, Br, I). Following this figure one can see that the dielectric constant at the static limit  $\varepsilon_1(0)$  depends upon the band gap of the compounds. There is an inverse relation between band gap and the values of the dielectric constant at the static limit  $\varepsilon_1(0)$ . This inverse relation can be explained by Peen Model [48]

$$\varepsilon(0) \approx 1 + (\hbar\omega_p / E_g)^2 \quad (17)$$

The energy band gap  $E_g$  can be calculated by the above equation by using the values of  $\varepsilon_1(0)$  and plasma energy  $\hbar\omega_p$ . It is clear from Fig. 13, 14, 15, 16, that  $\varepsilon_1(\omega)$  for CuX (X= F, Cl, Br, I), increases with the increase in energy to reach its maximum at about 9.0 eV, and 8.0 eV for CuF and CuCl, while for CuBr and CuI it reaches the maximum at 4.9 eV and 4.6 eV respectively, then it decreasing to negative value at about 11.50 eV for CuCl, whereas to about 8.50 eV and 7.50 eV for CuBr and CuCl respectively.

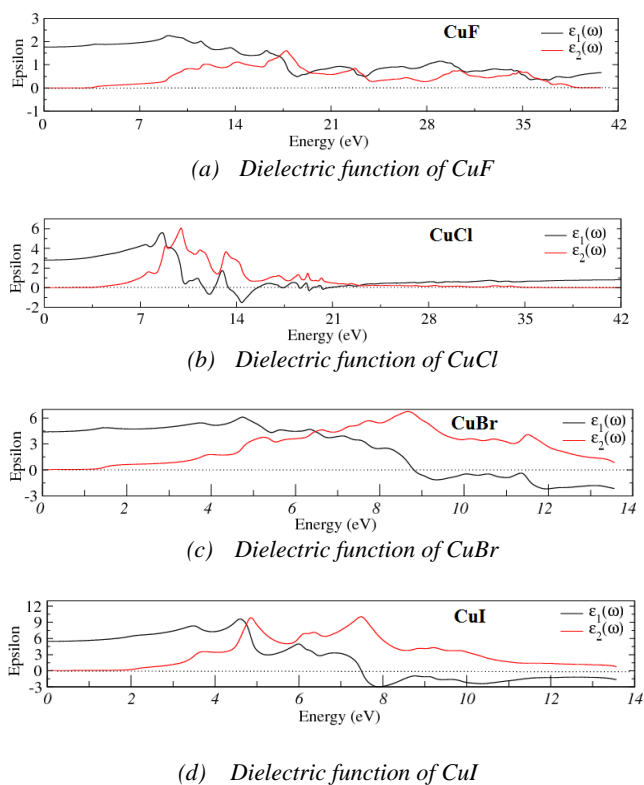


Fig. 10. Calculated dielectric functions of CuX (X= F, Cl, Br, I) compounds.

#### 4. Conclusion

Theoretical study of the structural, elastic, electronic and optical properties of copper halides are performed using FP-LAPW method within GGA, EV-GGA and mBJ potential. These compounds possess a direct band gaps ( $\Gamma$ - $\Gamma$ ), therefore these materials are widely used for optoelectronic devices. In the elastic constants it has been found that CuF and CuBr show brittle nature while CuCl and CuI show ductile behaviour. It is concluded that mBJ is an efficient theoretical technique for the calculation of the band gaps. The results expect that mBJ will be a successful tool for the band gaps engineering of IB-VIIA compounds. In these compounds, the peaks in the optical plots show the transition of electrons from valence band to the unoccupied states in the conduction band. From the analysis of optical spectra, it is predicted that these materials are useful for optical devices in the infrared, visible and ultraviolet energy ranges.

#### Acknowledgement

The result was developed within the CENTEM project, reg. no. CZ.1.05/2.1.00/03.0088, co-funded by the ERDF as part of the Ministry of Education, Youth and Sports OP RDI program. Computational resources were provided by MetaCentrum (LM2010005) and CERIT-SC (CZ.1.05/3.2.00/08.0144) infrastructures.

#### References

- [1] F. El Haj Hassan, A. Zaoui, W. Sekkal, Mater. Sci. Eng. B **87**, 40 (2001).
- [2] J. G. Gross, S. Lewonczuk, M. A. Khan, J. Rengeissen, Solid St. Commun. **36**, 907 (1980).
- [3] D. Westphal, A. Goldman, J. Phys. C, **15**, 6661 (1982).
- [4] Zaoui, Philosophical Magazine B, **82**(7), 791: 800 (2002).
- [5] B. Amrani, T. Benmessabih, M. Tahiri, I. Chiboub, S. Hiadsi, F. Hamdache: Physica B **381**, 179 (2006).
- [6] V. Meisalo, M. Kalliomaki, High Temp. High Pressures **5**, 663 (1973).
- [7] N. R. Serebryanaya, S. V. Popova, A. Rusakov, Sov. Phys. Solid State **17**, 1843 (1976).
- [8] R. Chelikousky, J. K. Burdett, Phys. Rev. Lett. **56**, 961 (1986).
- [9] K. S. Song, J. Phys., Paris, **28**, C3-43 195 (1976).
- [10] M. A. Khan, J. Phys. Chem. Solids, **31**, 2309 (1970).
- [11] A. Goldman, J. Tejeda, N. J. Shyevchik, M. Cardona, Phys. Rev. B, **10**, 4388 (1974).
- [12] A. Goldman, Phys. Stat. sol. (b), **81**, 9 (1977).
- [13] A. Zunger, M. L. Cohen, Phys. Rev. B, **20**, 1189 (1979).
- [14] L. Kleinman, K. Medinck, Phys. Rev. B, **20**, 2487 (1979).
- [15] A. B. Kunz, R. S. Weidman, J. Phys. C, **12**, L371 (1979).
- [16] A. J. Freeman, C. S. Wang, J. Jarlborg, M. Weinert, F. Wagner, C. W. Chu, J. quant. Chem., **13**, 445 (1979).
- [17] S. Ves, D. Golotzel, M. Cardona, H. Overfoh, Phys. Rev. B, **24**, 3073 (1981).
- [18] J. S. Wang, Y. M. Schluter, M. L. Cohen, Phys. Stat. sol. (b), **77**, 295 (1976).
- [19] P. V. Smith, J. Phys. Chem. Solids, **37**, 765 (1976).
- [20] H. C. Hsueh, J. R. Maclean, G. Y. Guo, M. H. Lee, S. J. Clark, G. J. Ackland, J. Crain, Phys. Rev. B, **51**(12) 216 (1995).
- [21] D. D. Koelling, B. N. Harmon, J. Phys. C: Solid State Phys. **10**, 3107 (1977).
- [22] P. Blaha, K. Schwarz, G. K. H. Madsen, D. Kvasnicka, J. luitz, Karlheinz Schwarz, Techn. Universitat, Wien, Austria, 2001, ISBN 3-9501031-1-2.
- [23] Z. Wu, R. E. Cohen, Phys. Rev. B **73**, 235116 (2006).
- [24] E. Engel, S. H. Vosko, Phys. Rev. B **47**, 13164 (1993).
- [25] F. Birch, Phys. Rev. **71**, 809 (1947).
- [26] S. Hull, D. Keen, Phys. Rev. B **50**, 5868 (1994).
- [27] R. C. Hanson, J. R. Hallberg, C. Schwab, Appl. Phys. Lett. **21**, 490 (1972).
- [28] G. J. Piermarini, F. A. Mauer, S. Block, A. Jayarman, T. H. Grballe, G. W. Hull, Solid State Commun. **32**, 275 (1979).
- [29] M. Hoffman, S. Hull, D. A. Keen, Phys. Rev. B **51**, 12022 (1995).
- [30] W. Sekkal, H. Aourag, M. Certier, J. Phys. Chem. Solids **59**(8), 1293 (1998).

- [31] G. Murtaza, Hayatullah, R. Khenata, M. N. Khalid, S. Naeem, *Physica B* **410**, 131 (2013).
- [32] V. Tvergaard, J. W. Hutshinson, *J. Am. Ceram. Soc.* **71**, 157 (1988).
- [33] W. Voigt, *Lehrbush der Kristallphysik*, Taubner, Leipzig, 1928.
- [34] A. Russ, *Angew. Mater. Phys.* **9**, 49 (1929).
- [35] Z. J. Wu, E. J. Zhao, H. P. Xiang, X. F. Hao, X. J. Liu, J. Meng, *Phys. Rev. B* **76**, 054115 (2007).
- [36] F. Peng, D. Chen, H. Fu, X. Cheng, *Phys. Status Solidi B* **246**, 71 (2009).
- [37] S. F. Pugh, *Philos. Mag.* **45**, 823 (1954).
- [38] A. Zaoui, M. Ferhat, M. Certier, H. Aourag, B. Khelifa, *Phys. Lett. A* **228**, 378 (1997).
- [39] O. Landolt-Bornstein, Springer, Berlin, **22**, 1986.
- [40] San-Guo Shen, *J. Phys. Condens. Matter* **6**, 8733 (1994).
- [41] R. C. Hanson, J. R. Hallberg, C. Schwab, *Appl. Phys. Lett.* **21**, 490 (1972).
- [42] W. Sekkal, A. Zaoui, A. Laref, M. Certier, H. Aourag, *J. Phys. Condens. Matter* **12**, 6173 (2000).
- [43] W. Kohn, L. J. Sham, *Phys. Rev. A* **140**, 1133 (1965).
- [44] J. P. Perdew, S. Burke, M. Ernzerhof, *Phys. Rev. Lett.* **77**, 3865 (1996).
- [45] A. Goldman, D. Westphal, *J. Phys. C*, **16**, 1335 (1983).
- [46] Roshan Ali, S. Mohammad, Hamid Ullah, S. A. Khan, H. Uddin, M. Khan, N. U. Khan, *Physica B* **410**, 93 (2013).
- [47] M. Fox, *Optical Properties of Solids* (Oxford University Press, New York, 2001).
- [48] D. Penn, *Phys. Rev.* **128**, 2093 (1962).

---

\*Corresponding author: hamidullah@yahoo.com  
hamidullah2k@yahoo.com